Space Weather of the Heliosphere: Processes and Forecasts
Proceedings IAU Symposium No. 335, 2017
C. Foullon & O.E. Malandraki, eds.

doi:10.1017/S1743921317010845

CCMC Modeling of Magnetic Reconnection in Electron Diffusion Region Events

Patricia H. Reiff[1], James M. Webster[1], Antoun G. Daou[1], Andrew Marshall[1], Stanislav Y. Sazykin[1], Lutz Rastaetter[2], Daniel T. Welling[3], Darren DeZeeuw[3], Maria M. Kuznetsova[2], Alex Glocer[2] and Christopher T. Russell[4]

[1]Rice Space Institute, Rice University, Houston, TX

[2]NASA Goddard Space Flight Center, Greenbelt, Maryland, USA

[3]Department of Atmospheric, Oceanic and Space Sciences, University of Michigan, Ann Arbor, Michigan, USA

[4]IGPP, University of California at Los Angeles, Los Angeles, CA

Abstract. We use numerical simulations from the Community Coordinated Modeling Center to provide, for the first time, a coherent temporal description of the magnetic reconnection process of two dayside Electron Diffusion Regions (EDRs) identified in Magnetospheric Multiscale Mission data. The model places the MMS spacecraft near the separator line in these most intense and long-lived events. A listing of 31 dayside EDRs identified by the authors is provided to encourage collaboration in analysis of these unique encounters.

Keywords. magnetic fields, methods: numerical, space vehicles: instruments, Earth, interplanetary medium, Sun: magnetic fields

1. Introduction

The Magnetospheric Multiscale Spacecraft (MMS) (Burch *et al.* 2015, 2016) provides unprecedented insights on magnetic reconnection, and its connection to microphysical processes occurring at Electron (EDR) and Ion (IDR) diffusion region scales. Through the Community Coordinated Modeling Center (CCMC), we ran the Space Weather Modeling Framework (SWMF) model (Powell *et al.* 1999; Tóth *et al.* 2005, 2012) including the Rice Convection Model (RCM) in highest resolution available (9.6 million cells) on several identified dayside EDR candidate events. This model provides additional insights on the global aspects of the reconnection process. For each case, we used measured solar wind and IMF data from OMNI data [http://omniweb.gsfc.nasa.gov/], propagated to the bow shock, and a steady Bx representing its average value for the 15-20 minutes before the time of the event. The SWMF at CCMC requires a steady Bx, and since we are modeling dayside events, the most recent IMF values were used; changing to a 30 or 45-minute Bx average would not have changed the results substantially. We then used the RECONX post processing tool (Glocer *et al.* 2016) to find the separator line and the positions of the magnetic nulls.

2. Modeling the EDR Events

We present field lines traced from CCMC models of two of the dayside EDR events analyzed in detail in Webster *et al.* (2017): January 10 and November 23, 2016. The full list of the 31 candidate EDR events, based on the presence of electron crescents and significant agyrotropy (Swisdak 2016), is given in Table 1. The two time periods

Table 1. 31 Dayside EDR Candidate Events.

Event	Date & Time (UTC)	X_{GSM} (R_E)	Y_{GSM} (R_E)	Z_{GSM} (R_E)	Separation (km)	$(j \cdot E')_{max}$ $nW.m^{-3}$	$(\sqrt{Q_e})_{max}$ index
A01	09/19/2015 07:43:30	6.346	5.399	-2.982	71.57	6.05	0.060
A02	10/16/2015 10:33:30	9.231	6.092	-4.403	13.87	2.42	0.052
A03	10/16/2015 13:07:02	8.310	7.078	-4.800	13.78	22.57	0.090
A04	10/22/2015 06:05:22	9.637	3.481	-1.961	16.93	7.47	0.069
A05	11/01/2015 15:08:06	7.814	6.202	-3.470	14.58	4.15	0.072
A06	12/06/2015 23:38:31	8.516	-3.916	-0.810	19.23	10.13	0.066
A07	12/08/2015 11:20:44	10.233	1.288	-1.364	15.30	8.31	0.084
A08	12/09/2015 01:06:11	9.922	-3.671	-0.928	17.34	1.07	0.051
A09	12/14/2015 01:17:40	10.131	-4.163	-1.191	16.97	7.13	0.095
A10	01/07/2016 09:36:15	8.888	-1.968	-0.733	41.75	6.78	0.047
A11	01/10/2016 09:13:37	8.808	-2.395	-0.775	40.84	13.98	0.066
A12	02/07/2016 20:23:35	3.874	-9.325	-5.720	15.99	0.38	0.057
B13	10/22/2016 12:58:41	6.406	7.700	-4.706	8.87	11.92	0.055
B14	11/02/2016 14:46:18	7.241	8.812	-3.543	8.18	1.09	0.036
B15	11/06/2016 08:40:58	7.943	4.113	-2.826	11.76	8.12	0.075
B16	11/12/2016 17:48:47	6.624	9.165	-1.104	7.35	5.12	0.048
B17	11/13/2016 09:10:41	8.958	4.563	-2.625	11.38	18.28	0.050
B18	11/18/2016 12:08:11	9.596	6.460	-2.509	4.88	1.02	0.050
B19	11/23/2016 07:49:33	9.613	3.232	-1.604	6.43	7.35	0.121
B20	11/23/2016 07:49:52	9.613	3.232	-1.604	6.43	32.32	0.089
B21	11/23/2016 07:50:30	9.620	3.245	-1.608	6.42	8.57	0.078
B22	11/28/2016 15:47:00	8.884	7.184	-0.440	6.32	1.63	0.036
B23	12/11/2016 04:41:50	9.489	-0.056	-0.448	6.89	2.07	0.026
B24	12/19/2016 14:15:02	10.204	4.170	0.934	8.42	2.33	0.050
B25	01/02/2017 02:58:13	9.647	-3.007	-0.649	9.96	2.37	0.026
B26	01/11/2017 04:22:43	10.809	-3.713	-0.154	8.17	8.53	0.055
B27	01/20/2017 12:32:07	9.634	-0.461	1.967	6.47	8.31	0.051
B28	01/22/2017 10:15:46	10.744	-2.138	1.766	5.75	4.13	0.043
B29	01/22/2017 10:15:58	10.750	-2.148	1.764	5.74	3.39	0.044
B30	01/22/2017 10:47:33	10.519	-1.790	1.837	5.86	1.98	0.036
B31	01/27/2017 12:05:43	9.270	-1.370	1.964	6.05	7.51	0.046

(corresponding to four events) modeled here were chosen because of their high values of electric fields and agyrotropy.

In the 9.6M cell adaptive grid used here, the effective grid spacing near the dayside magnetopause is 0.125 R_E (Tóth *et al.* 2005). The color contour shows the particle pressure at X_{SM}=10 R_E (near the location of MMS in both events for Fig 1 (A-E) and Fig 2 (F-J); for Fig 2 A-E, the pressure is shown at a location of Y_{SM} = 3.5 R_E, again near the MMS location. Fig 1 shows the field line tracing for January 10, using

https://doi.org/10.1017/S1743921317010845 Published online by Cambridge University Press

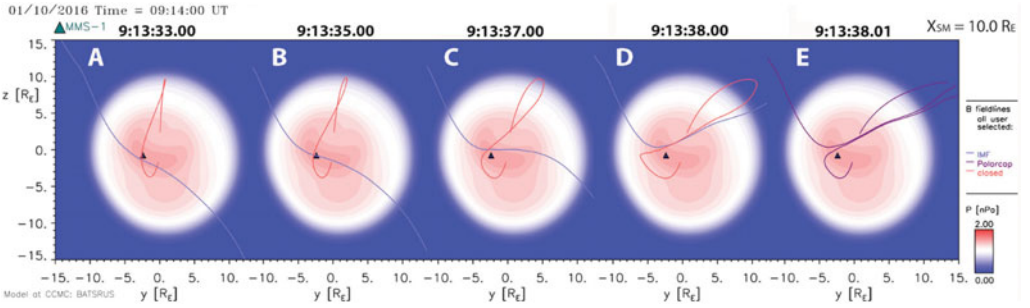

Figure 1. Time sequence for January 10, 2016, showing the plane at X_{SM} =10 R_E. The color indicates particle pressure in that plane. An .mp4 movie including these frames and more can be found in the supplemental material accessible at Cambridge's CJO site: journals.cambridge.org and also at http://mms.rice.edu/mms/Publications/IAU_335/.

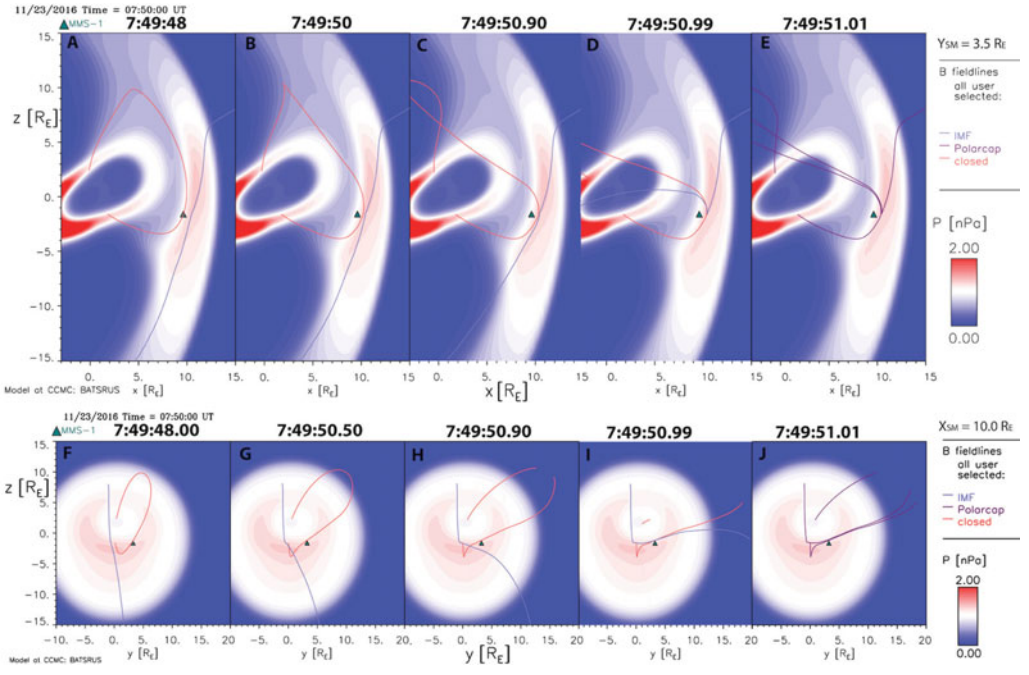

Figure 2. Field lines and particle pressures shown in Y_{SM} =3.5 R_E plane (A-E) and in the X_{SM} =10 R_E plane (F-J) for the EDR events on November 23, 2016. The color contours indicate the particle pressure in that plane. CCMC Run: James Webster_032117_1. Modeling time step for all of the panels is 07:50:00 UT. Two mp4 movies, one each for the two plane views, including these frames and more can be found in the supplemental material accessible at Cambridge's CJO site: journals.cambridge.org and also at http://mms.rice.edu/mms/Publications/IAU_335/

the model run (James_Webster_090216_1). All of the tracings shown here are done for a single time step of the model (09:14). The newly reconnected field lines closest to MMS were found (E), and then, by using the modeled velocity of the northward extension of that open field line, we map its position backwards in time in the previous panels (the blue IMF line from top left to bottom right in panels A-D). Thus the times in each panel are accurate relative times. Note that the IMF does have a substantial By component at the beginning (A), but both the solar wind field lines (blue) and closed magnetospheric field lines (red) exhibit a strongly enhanced By component just before reconnection (D)

https://doi.org/10.1017/S1743921317010845 Published online by Cambridge University Press

and just after (E), consistent with the MMS observations. In only 3 seconds the field line undergoes profound stretching as it approaches the reconnection site, and requires only 0.01 second to reconnect. Movies showing these frames and additional frames can be found at http://mms.rice.edu/MMS/publications/IAU_335/ . Fig 2 shows field tracings from the November 23 event, which was actually three encounters with EDRs in Table 1. Looking from the side at the location of MMS (y = 3.5 R_E), the reconnecting fields look nearly two-dimensional (panels A-C), but in D, the field mapping from the northward sheath takes a sharp turn into the y-direction as the IMF field line (blue) nears the dayside null. The lower set of panels are viewed parallel to the YZ plane at a cut near the MMS spacecraft location.

The IMF field line makes nearly a 90° turn at the null point (panel I) as the southern end of the field line continues downstream. The fact that MMS is located very near the separator is likely the reason that it observed three very intense EDR candidates in the space of a single minute (Webster *et al.* 2017). The relative timings on the plot are calculated from the flow velocities in the solar wind, so are accurate on solar wind and open field lines but approximate for the closed field lines. The MMS flow data suggest that the MMS location switches back and forth from below to above the X-line, consistent with remaining in the location of the separator for an extended time.

One striking result seen these two examples is the extreme distortion of both the closed and solar wind field lines as they near the reconnection point. Both field lines take on an induced guide field. This induced guide field is consistent with the solar wind field line being "hung up" on the dayside nose and being stretched as both ends continue to propagate downstream. The surprising result (at least to us) is that the interior field line also stretches to meet the exterior field line so that, at the exact time of reconnection, the interior closed field line and the exterior solar wind field line are actually parallel, allowing flow across the open/closed boundary. Numerical diffusion in the model allows a parallel electric field to break the frozen field condition along that line. Thus, multiple encounters seen on November 23 could be associated with temporally variable reconnection or several reconnection locations along the separator line, or motion of the separator in and out of the spacecraft suite.

Although we found the reconnection lines by interrogating the model near the position of MMS, we also ran the "RECONX" model (not shown) to postprocess the model results to find the null points and the separator line for each of these events. Not surprisingly, RECONX found the separator line to be along the stretched portion of the reconnecting field lines, with one null point on the dayside near MMS and the other null point typically in the magnetotail. In these events (January 10 and November 23, 2016), MMS was not only very near the separator, but also only a few R_E away from the dayside null point. This may explain why these two events have some of the largest electric fields, currents, and agyrotropies of the entire EDR data set.

3. Conclusions

This paper presents the first estimates of the field line travel times through realistic reconnection simulations. The simulation shows clearly how an induced guide field makes the reconnecting field lines parallel to the separator line. This distortion occurs in the last one to three seconds before reconnection. The length of time a given flux tube remains in the reconnection region is extremely small (hundredths to thousandths of seconds). The models predict severe configuration changes on the scale size of an electron gyroradius near the separator line. This paper also presents the importance of using fully 3D reconnection, including separator lines, on the dayside magnetopause.

https://doi.org/10.1017/S1743921317010845 Published online by Cambridge University Press

4. Acknowledgements

The authors thank the MMS team for an amazing suite of instruments. This work was carried out using the SWMF tools developed at The University of Michigan's Center for Space Environment Modeling (CSEM), and RECONX developed by NASA. These tools are made available through the NASA Community Coordinated Modeling Center (CCMC). This work also used plasma and IMF data through CDAWEB. This study was supported by NASA under grant NNX14AN55G.

References

Burch, J. L., Moore, T. E., Torbert, R. B. & Giles, B. L. 2015, *Space Sci. Rev.*, doi:10.1007/s11214-015-0164-9

Burch, J. L. Torbert, R. B., *et al.* 2016, *Science*, 352, doi: 10.1126/science.aaf2939

Glocer, A., Dorelli, J., Toth, G., Komar, C. M. & Cassak, P. A. 2016, *J. Geophys. Res.*, Vol: 121, Pages: 140-156; doi:10.1002/2015JA021417

Powell, K. G., Roe, P. L., Linde, T. J., Gombosi, T. I. & De Zeeuw, D. L. 1999, *J. Comput. Phys.*, 154 (2), 284, doi:10.1006/jcph.1999.6299

Swisdak, M. 2016, *Geophys. Res. Lett.*, 43, 43-49, doi:10.1002/2015GL066980

Tóth, G. Sokolov, I. V., *et al.* 2005, *J. Geophys. Res.*, 110, A12226. doi: 10.1029/2005JA011126

Tóth, G., van der Holst, B., Sokolov, I. V., *et al.* 2012, *J. Comput. Phys.*, 231, 870, doi:10.1016/j.jcp.2011.02.006

Webster, J. Burch, J., *et al.* 2017, *J. Geophys. Res.*, submitted